ELSEVIER

Wave Motion 20 (1994) 83–87

WAVE MOTION

Imaging of group velocity surfaces in a cuspidal region of zinc by laser-generated ultrasonic waves

Kwang Yul Kim

Department of Theoretical and Applied Mechanics, Thurston Hall, Cornell University Ithaca, New York 14853, USA

Received 15 September 1993, Revised 24 January 1994

Abstract

An image of group velocity surfaces within and outside a cuspidal region of a (0001) oriented zinc crystal is obtained with a pointlike scanning laser source and a fixed longitudinal (L) mode piezoelectric detector. Because of axisymmetric excitation and sensing, the group velocity surface of the pure transverse (PT) mode, being shear horizontally (SH) polarized, is absent in the obtained image. In the cuspidal region the quasi transverse (QT) mode has three group velocity branches in a given direction: the fast QT (FQT) branch, the intermediate speed QT (IQT) branch, and the slow QT (SQT) branch. The laser imaging clearly shows the wave fronts of the quasi longitudinal (QL), IQT, and SQT rays in the cuspidal region. Near the epicentral [0001] direction, the arrivals of the head wave (HW) and SQT rays are almost simultaneous and their wave fronts are not distinct. However, farther from the epicentral direction, they separate and outside the cuspidal region the imaging shows the group velocity surfaces of the QL, HW, and SQT rays.

1. Introduction

In anisotropic media such as transversely isotropic composites and zinc crystal, the phase and group velocities in general do not coincide with each other. In a general direction of propagation, there are three wave modes traveling at distinct velocities, one quasi longitudinal (QL) and two quasi transverse (QT) modes, with their polarizations mutually perpendicular to each other. Elastic waves generated by excitation of a broadband source propagate at the speed of the group velocity. The pulsed excitation of a pointlike source gives rise to the elastic waves propagating in virtually all directions.

In this experiment we used a pulsed laser beam focused on the upper surface of a disk-shaped, 25.8 mm thick zinc crystal oriented in the (0001) plane to generate a broadband pointlike source of acoustic emission. A small longitudinal (L) mode piezoelectric transducer fixed at the center of the bottom surface detected the various ultrasonic wave modes that traveled from the source at their own distinct group velocities. The detection of various QL and QT modes propagating in a wide range of directions is carried out by scanning the laser beam across the epicenter on the upper surface. A group velocity image is constructed from the detected signals, whose ray directions span from the symmetry direction beyond the cuspidal region.

2. Theoretical background

The group or ray velocity $\mathbf{V}_g$ is obtained from the relation [1]

$$\mathbf{V}_g \equiv \nabla_{\mathbf{k}}\omega = \nabla_{\mathbf{n}}V = \frac{\nabla_s \Lambda}{\mathbf{s}\cdot\nabla_s\Lambda}, \tag{1}$$

SSDI 0165-2125(94)00013-U

where ω is the angular frequency, $\mathbf{k}$ the wave vector, $\mathbf{n}=\mathbf{k}/|\mathbf{k}|$ the wave normal, V the phase velocity, $\mathbf{s}$ the slowness defined as $\mathbf{n}/V$, and Λ the equation of the slowness surface. The above equation indicates that the outward normal to the slowness surface at any point is the direction of energy flux or group velocity of the corresponding mode. The fourth rank elastic stiffness tensor C_{ijkl} of a hexagonal or transversely isotropic medium is characterized by five elastic constants: C_{11}, C_{33}, C_{44}, C_{12}, and C_{13}. For zinc they have been measured to be $C_{11}=163.75$ GPa, $C_{33}=62.93$ GPa, $C_{44}=38.68$ GPa, $C_{12}=36.28$ GPa, and $C_{13}=52.48$ GPa.

The (010) section of slowness surfaces of zinc is shown in Fig. 1, which displays three sheets belonging to the QL, pure transverse (PT), and QT modes. We simplify the directional notation [0001] of a hexagonal crystal to [001] that is appropriate for transversely isotropic media including some composite materials. In crystallography, $[hkl]$ zone represents the set of planes that are all parallel to the $[hkl]$ direction, where h, k, and l are natural numbers. For a transversely isotropic zinc crystal, all the planes belonging to the [001] zone are identical and the (010) plane is a typical representation of the [001] zonal plane. For a $\mathbf{k}$ along an arbitrary direction in the zonal plane, one of the QT modes, say, the QT 1 becomes a PT mode which is shear horizontally (SH) polarized parallel to the basal plane (001) and normal to the zonal plane. Both QL and QT 2 modes are polarized in the sagittal plane coinciding with the zonal plane. Hence, we simply denote QT 1 and QT 2 as PT and QT, respectively.

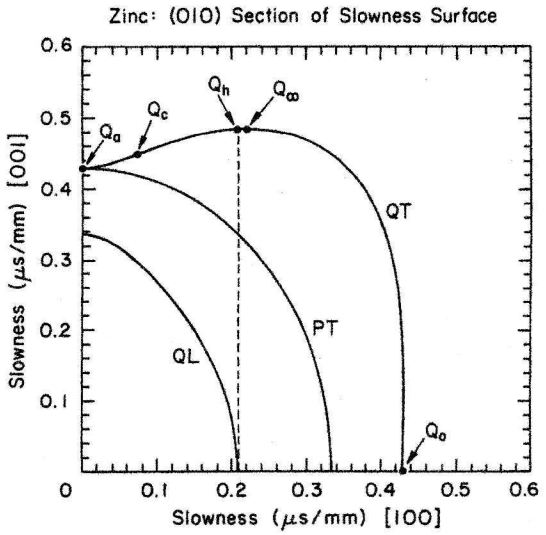

Fig. 1. (010) section of slowness surfaces in zinc.

Shown in Fig. 2 are the corresponding group velocity (or ray) surfaces obtained using Eq. (1). For zinc the QT wave in the various [001] zonal planes propagates at a phase velocity slower than that of the PT wave. For this reason the QT mode is sometimes called the slow transverse (ST) mode and the PT mode is dubbed the fast transverse (FT) mode. However, for the group velocity surfaces in the cuspidal region, this distinction is somewhat blurred, as one can see that the QT group velocity surface penetrates through the PT group velocity surface. The cuspidal feature shown in Fig. 2 arises due to a particular shape of the QT mode slowness surface shown in Fig. 1. Around the symmetry axis [001] it is concave with both principal curvatures being negative. At point Q_c the principal curvature in the zonal plane changes sign and the surface is saddle-shaped from Q_c to the point Q_∞ where the principal curvature transverse to the zonal plane changes sign and the normal to the surface points in the symmetry direction [001]. There is a band on either side of the basal plane near Q_0 where the in-plane curvature of the slowness surface is negative, giving rise to an inplane cusp about point P_0 in the basal plane of the corresponding group velocity surface. This cusp is, however, too small to be seen in the scale of drawing of Fig. 2 and can be seen only in a greatly magnified view [2,3]. It cannot be detected with the time resolution of this experiment and we will not discuss it further. In Fig. 2, the points P_a and P_∞ on the symmetry axis, the cuspidal edge P_c and the point P_0 on the basal plane correspond to the points Q_a, Q_∞, Q_c, and Q_0 in Fig. 1, respectively. For simplicity of nomenclature let us call the ray

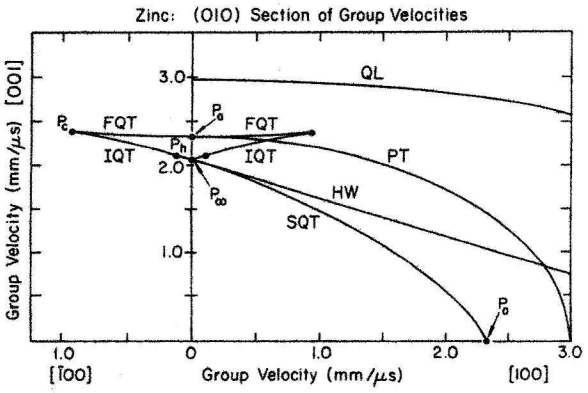

Fig. 2. (010) section of group velocity surfaces in zinc.

branches of QT mode, P_aP_c, P_cP_∞, and $P_\infty P_0$ by their acronyms, FQT (fast QT), IQT (intermediate QT), and SQT (slow QT) branches, respectively.

Explicit analytical expressions for the group velocity of QL, PT and QT modes as a function of an arbitrary direction in the zonal plane are given by Kim [3]. Analytical relations between the directions of wave normal **n** and the corresponding group velocity are found in Refs. [1] and [3]. Using these relations found in Refs. [1] and [3], the directions of the cuspidal edge P_c in Fig. 2 and the conical surface OQ_∞ in Fig. 1 are calculated to be 21.54° and 24.52° from the symmetry direction, respectively. The mirror images of the FQT and IQT branches across the [001] axis, which correspond to the wave normals on the QT slowness sheet reflected across the [001] axis in Fig. 1, are also drawn in the first quadrant of Fig. 2. Since a broadband pointlike source including the laser source used in this experiment generates wave normals in virtually all directions, these mirror images of the group velocity branches may actually be observable together with other possible modes.

The head wave observed by the detector is not generated by the laser source. It is brought about by mode conversion. The L waves traveling from the source on the free surface continuously radiate a part of their energy to meet the free boundary conditions and the wave front of these interior rays is known as a head wave, which propagates as a QT mode that is sagittally polarized. The tangential component of the slowness of the head wave at the free surface should match that of the L mode, which is the slowness of the QL mode along the [100] direction in Fig. 1. The measured group velocity of the L wave traveling along the surface equals 4791 m/s. The slowness of the mode-converted head wave is denoted by the point Q_h in Fig. 1, which makes an angle of 23.28° from the symmetry axis, when viewed from the origin. The group velocity at the point Q_h of the slowness surface corresponds to the point P_h on the IQT branch of the group velocity surface shown in Fig. 2. The direction of the head wave is that of the OP_h, which makes an angle θ_h equal to 3.04° with the symmetry direction. The group velocity of the head wave OP_h is calculated to be 2113 m/s. Unlike the head wave in an isotropic media, the direction of which usually makes an acute angle with that of the L wave traveling on a free surface, the head wave in zinc makes an obtuse angle 93.04° from the corresponding L wave.

As a result, the head waves arriving at the detector from an epicentral laser source constitute a cone of half-apex angle 3.04°, while for an off-epicentral laser source, the head wave front arriving at the detector is no longer conic. The L wave traveling on the surface from the off-epicentral source passes through the epicenter, continuously shedding parts of its energy on its way as head waves. Only the head wave generated at the point, the direction of which toward the detector makes the angle θ_h (= 3.04°) with the symmetry axis, arrives at the detector. These head wave paths are illustrated in Fig. 3.

Denoting the distance of the laser source from the epicenter by x and the specimen thickness by h (refer to Fig. 3), the head wave arrival time t_h is given by

$$t_h = \frac{x + h\sin\theta_h}{4791} + \frac{h}{2113\cos\theta_h} \tag{2}$$

The equivalent group velocity corresponding to the arrival of the head wave, V_{gh}, is

$$V_{gh} = \frac{\sqrt{x^2+h^2}}{t_h}. \tag{3}$$

Eq. (3) is plotted in Fig. 2 and marked with HW (head wave). A detailed description of the head wave in transversely isotropic media is given by Musgrave and Payton [4].

As seen in Fig. 2, near the epicenter, the arrivals of the head wave and SQT ray are almost simultaneous. At the epicenter the arrival of the head wave is calculated to be only 0.010 μs ahead of the arrival of the

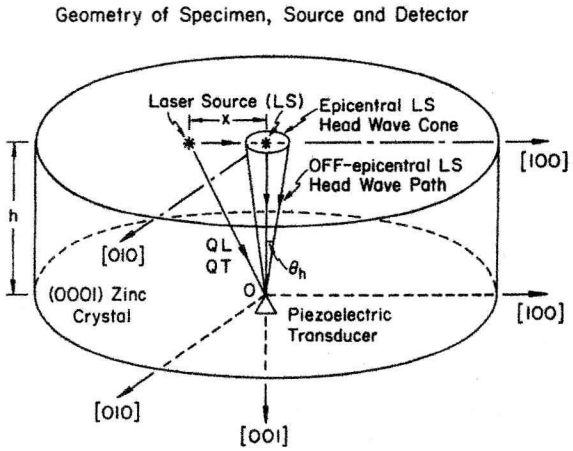

Fig. 3. Geometry of specimen, source, detector, and ray paths to the detector.

SQT ray. Taking into account the sampling time of 0.0167 μs and the finite size of detector (1.3 mm diameter), both arrivals are considered as simultaneous within experimental error. However, the farther the laser source moves from the epicenter, the more gradually they separate and the head wave arrives appreciably earlier than the SQT ray. For example, at the 14 mm laser source position from the epicenter, the head wave is supposed to arrive 0.90 μs ahead of the arrival of the SQT ray.

3. Laser scan imaging

Fig. 3 shows a schematic of the geometry of specimen, laser source (LS), L mode piezoelectric detector, and some of the ray paths including those of the head waves. The specimen is a disk-shaped, (001) oriented zinc crystal with its basal diameter 75 mm and thickness 25.8 mm. The detector is fixed at origin on the bottom basal plane, while a pulsed high-intensity laser beam focused on the top surface is scanned across the epicentral position on the straight line in the range of −20 mm to 20 mm from the epicenter. The laser source duration is typically several ns. The detected signals are first amplified with 40 dB gain by an amplifier, the bandwidth of which extends from 100 kHz to 10 MHz, and fed into a digitizer which samples the amplified outputs at a rate of 60 MHz. The digitized output is also connected to an x–y scope for visual display and brought into a digital computer for subsequent signal processing and image construction.

Shown in Fig. 4a is a scan image thus obtained, which manifests group velocity fronts of various modes including QL, IQT, SQT, and HW modes. It is seen in the figure that the output of the thin-disk shaped piezoelectric detector rings for a while after each ray arrival. In the image the 10 mm scan position approximately corresponds to the cuspidal edge P_c in Fig. 2. Arrival times of the sagittally polarized rays including QL, HW, FQT, IQT, and SQT rays, which travel from the source to the detector, are calculated using the group velocities shown in Fig. 2 and they are plotted in Fig. 4b for various laser scan positions. Fig. 4b is drawn exactly in the same scale as Fig. 4a for direct comparison between them, which indicates that the arrivals of observed group velocity wave fronts of various modes are in excellent agreement with those predicted by theory.

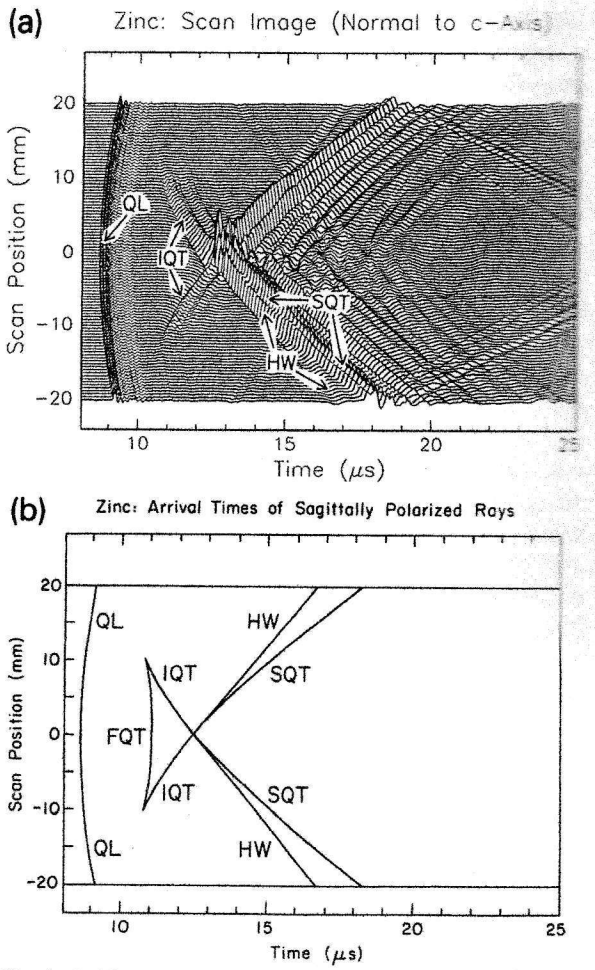

Fig. 4(a). Observed laser scan image of group velocity surfaces in zinc. (b). Calculated arrival times of sagittally polarized rays for various scan positions in zinc.

The arrival of the FQT ray causes a small discontinuity in the slope of a theoretical displacement signal [2,5], which may well become smooth in an experimental signal because of the finite size of source and detector, and finite bandwidth of the whole experimental system. This makes the detection of the FQT wave difficult by the thin-disk shaped piezoelectric detector that is principally sensitive to a change in the normal component of a surface displacement. Indeed, in the laser scan image the FQT wave front is not visible. However, it can be seen in the displacement signal detected by the capacitive transducer very near the first zero crossing after the QL mode arrival [6]. The absence of the PT mode in the scan image is because of axisymmetry of the thermoelastic laser source and

L mode detector associated with the specimen oriented in the symmetry plane (001). The axisymmetric nature of the source results in a net displacement being zero in the transversely isotropic plane (001). The PT mode, being SH polarized, is neither generated nor detected. Direct determination of the entire group velocity surfaces including those of the FQT and PT modes is reported elsewhere [6]. The small ripples found running diagonally after the QL mode arrival in the signals obtained at offepicentral laser source positions between 12 and 20 mm are apparently caused by the arrival of the L mode signals reflected from the side walls of the finite sized specimen.

The large amplitude of the SQT ray associated with the high peaked ridge at the epicenter is due to strong focusing, toward the symmetry direction, of all the QT modes with their **k** vectors lying on the circular cone generated by rotating the OQ_∞ (see Fig. 1) around the symmetry axis. All these QT modes have the same ray vector located on the conical point P_∞ in Fig. 2 and have their acoustic energy directed along the symmetry direction. The large amplitude of the SQT ray rapidly diminishes as the laser source moves a small distance from the epicenter. This is known as a phenomenon of phonon focusing and the observation of phonon focusing in zinc at ultrasonic frequencies is reported by Kim et al. [7]. Note that at point Q_∞ the Gaussian curvature of the slowness surface is zero, and therefore the theoretical phonon focusing factor at Q_∞ is infinite [8]. The large amplitude of the epicentral SQT ray overwhelms weakly focused conical head waves that arrive almost simultaneously at the detector as mentioned in the previous section. A quantitative theoretical treatment of the contribution of the SQT and HW rays to an epicentral motion in zinc is described elsewhere [2,9].

4. Conclusions

We have demonstrated that a laser scan image reveals the various group velocity fronts within and outside a cuspidal region in zinc. Those of QL, IQT, SQT and HW waves are clearly shown in the image in excellent agreement with those predicted by theory. The image shows two cuspidal branches, which are those of IQT and SQT modes. Due to axisymmetry of the laser source and the characteristics of the thin-disk shaped piezoelectric detector, neither PT nor FQT modes are visible in the scan image.

Acknowledgement

I am deeply grateful for the financial support from the Physical Acoustics Division of the Office of Naval Research. My thanks are also due to B.F. Addis, who provided me with a large zinc single crystal of fine quality.

References

[1] M.J.P. Musgrave, *Crystal Acoustics*, Holden-Day, San Francisco (1970).
[2] R.G. Payton, *Elastic Wave Propagation in Transversely Isotropic Media*, Martinus Nijhoff, The Hague (1983).
[3] K.Y. Kim, "Analytic relations between the elastic constants and the group velocity in an arbitrary direction of symmetry planes of media with orthorhombic or higher symmetry", *Phys. Rev. B* 49, 3713–3724 (1994).
[4] M.J.P. Musgrave and R.G. Payton, "Head wave contributions to elastic wave fields in a transversely isotropic half-space", *Q.J. Mech. Appl. Math.* 34, 235–250 (1981).
[5] A.G. Every and K.Y. Kim, "Time domain dynamic response functions of elastically anisotropic solids", *J. Acoust. Soc. Am.* 95, 2505–2516 (1994).
[6] K.Y. Kim and W. Sachse, "Direct determination of group velocity surfaces in a cuspidal region in zinc", *J. Appl. Phys.* 75, 1435–1441 (1994).
[7] K.Y. Kim, W. Sachse and A.G. Every, "Focusing of Acoustic Energy at the Conical Point in Zinc", *Phys. Rev. Lett.* 14, 3443–3446 (1993).
[8] H.J. Maris, "Enhancement of heat pulses in crystals due to elastic anisotropy", *J. Acoust. Soc. Am.* 71, 812–818 (1971).
[9] R.G. Payton and M.J.P. Musgrave, "Axial motion of a transversely isotropic elastic half-space in which the head wave and conical point arrival times coincide", *J. Elasticity* 13, 149–155 (1983).